

Hinode Calibration for Precise Image Co-alignment between SOT and XRT (November 2006 – April 2007)

Toshifumi SHIMIZU¹, Yukio KATSUKAWA², Keiichi MATSUZAKI¹, Kiyoshi ICHIMOTO², Ryohei KANO², Edward E. DELUCA³, Loraine L. LUNDQUIST³, Mark A. WEBER³, Theodore D. TARBELL⁴, Richard A. SHINE⁴, Mitsuru SÔMA², Saku TSUNETA², Taro SAKAO¹, and Kenji MINESUGI¹

¹*Institute of Space and Astronautical Science (ISAS), Japan Aerospace Exploration Agency (JAXA),
3-1-1 Yoshinodai, Sagamihara, Kanagawa, 229-8510
shimizu.toshifumi@isas.jaxa.jp*

²*National Astronomical Observatory of Japan, Mitaka, Tokyo 181-8588*

³*Harvard-Smithsonian Center for Astrophysics, Cambridge, MA 02138, U.S.A.*

⁴*Lockheed Martin Solar and Astrophysics Laboratory, Bldg. 252, 3251 Hanover St., Palo Alto, CA 94304, U.S.A.*

(Received 2000 December 31; accepted 2001 January 1)

Abstract

To understand the physical mechanisms for activity and heating in the solar atmosphere, the magnetic coupling from the photosphere to the corona is an important piece of information from the Hinode observations, and therefore precise positional alignment is required among the data acquired by different telescopes. The Hinode spacecraft and its onboard telescopes were developed to allow us to investigate magnetic coupling with co-alignment accuracy better than 1 arcsec. Using the Mercury transit observed on 8 November 2006 and co-alignment measurements regularly performed on a weekly basis, we have determined the information necessary for precise image co-alignment and have confirmed that co-alignment better than 1 arcsec can be realized between Solar Optical Telescope (SOT) and X-Ray Telescope (XRT) with our baseline co-alignment method. This paper presents results from the calibration for precise co-alignment of CCD images from SOT and XRT.

Key words: Sun: photosphere - chromosphere, Sun: corona – X-rays, gamma rays, space vehicles: instruments, methods: data analysis

1. Introduction

Many of the observational studies by the Hinode spacecraft to address magnetic couplings in the solar atmosphere need to combine the data from some of the three telescopes onboard the spacecraft (Kosugi et al. 2007). After its successful launch and its early operation, the Solar Optical Telescope (SOT, Tsuneta et al. 2007; Tarbell et al. 2007; Suematsu et al. 2007; Shimizu et al. 2007; Ichimoto et al. 2007) has started to produce series of 0.2–0.3 arcsec visible-light images, giving the dynamical behavior of solar magnetic fields on the solar surface. Simultaneously, the X-ray Telescope (XRT, Golub et al.; Kano et al. 2007) has been providing 1 arcsec resolution X-ray images of the solar corona, giving the location of heating and dynamics occurring in the corona. Precise image co-alignment of SOT and XRT data with sub-arcsec accuracy (0.5 arcsec as our goal) is required to provide new information regarding magnetic couplings from the photosphere to the corona.

The satellite structure was designed with careful consideration to meet the telescope alignment requirements: the 1 hour stability must be 5 arcsec (0-p), and the static DC offset in the pointing of each telescope must be 80 arcsec (0-p), to allow telescopes with narrow fields of view to observe the same observing target. Here the static DC off-

set means the static deviation on the pointing direction of one telescope from that of the other telescope on orbit after experiencing the launch mechanical environment. The sub-arcsec accuracy required on the image co-alignment is realized with calibration using scientific images acquired during the flight. The three telescopes are aligned along the Z axis of the spacecraft and supported by an optical bench unit (OBU). The OBU is a cylinder made up of composite material that internally supports the optical telescope part (OTA; Suematsu et al. 2007) of the SOT. The SOT's focal plane package (FPP; Tarbell et al. 2007), EIS (EUV imaging spectrometer, Culhane et al. 2007) and XRT are kinematically mounted on the outside of the OBU with 6 mounting legs each, which constrain the degrees of freedom of the rigid body. The OBU also holds a tower to whose upper surface the sun sensors are attached.

For achieving sub-arcsec accuracy in co-aligning the images to each other, a baseline co-alignment concept adapted to the Hinode data was defined in the early phase of the spacecraft development, which is briefly summarized in section 2. After each telescope started initial observations in late October 2006, the DC pointing offsets among the telescopes were determined with the data acquired during the Mercury transit on the solar disk. This provides us with a unique calibration opportunity; we are

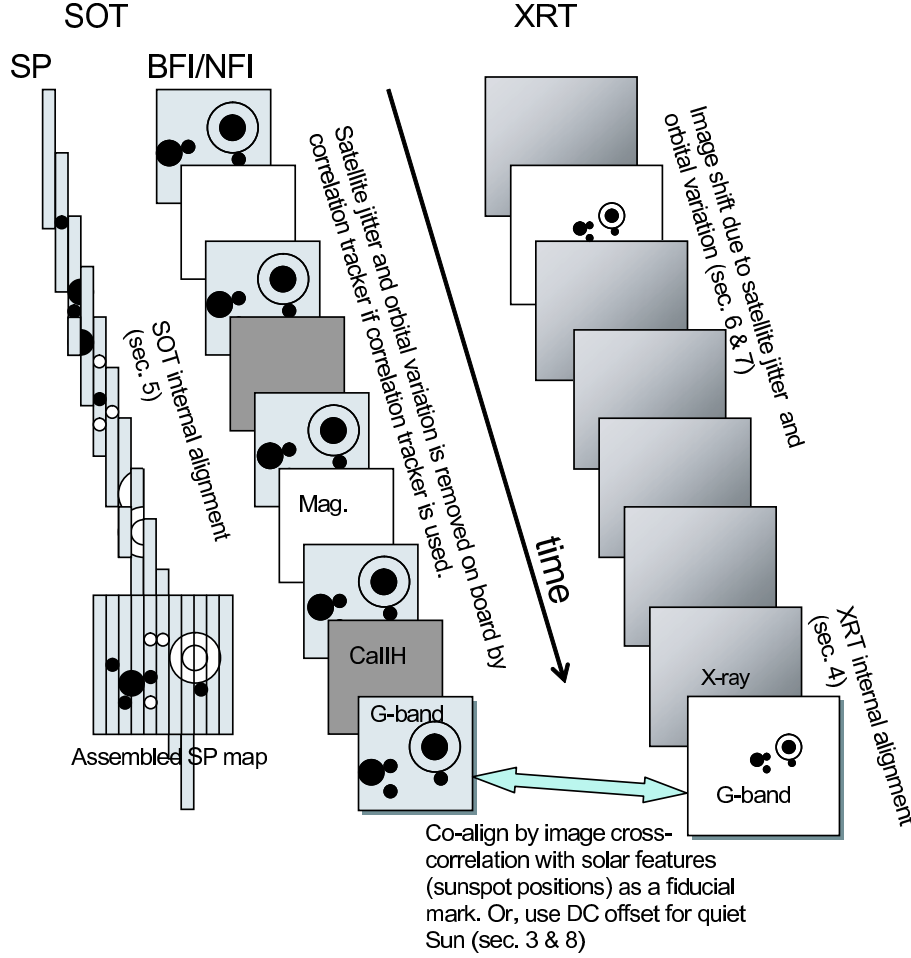


Fig. 1. Schematic explanation of the baseline method for the most accurate co-alignment of the Hinode data.

able to accurately determine the DC pointing offset, the plate scale, and the roll angle of the CCD images from solar north (section 3). The XRT can take both G-band images, through the Visible Light Imager, and X-ray images; the offsets between these two imaging systems are discussed in section 4. Similarly for SOT, images taken through different filters are slightly offset from each other, as discussed in section 5. The pointing direction of each telescope slightly varies with time, primarily associated with the orbital phase of the satellite. Section 6 shows how the pointing direction of each telescope and sun sensors changes with orbital phase. This information is used when the time series of XRT images is co-aligned. Section 7 describes the method using the orbital variation model and sun sensor signals to remove the satellite jitter and longer time drift due to orbital variation. This alignment method is shown to give excellent performance, i.e., residual jitter of 0.3 arcsec at the 1σ level or better. Finally, section 8 shows how the DC offset between SOT and XRT pointing varies from November 2006 to April 2007. This information can allow us to establish a more general method for co-alignment between SOT and XRT if we correctly manage the behavior of the tip-tilt mirror in SOT. The general method is crucial for quiet Sun studies.

This paper does not discuss the co-alignment of SOT and XRT with data from EIS, which observes EUV spectral lines with slit or slot scanning of an observing region for diagnosing the properties of the plasma in the transition region and lower corona. This is because we need more calibration efforts to register the assembled scans of EIS spectral data to the rigid CCD frames from XRT and SOT. The co-alignment of SOT and XRT with EIS data will be presented in a separate paper after completing the calibration efforts.

2. SOT/XRT co-alignment method

The baseline method for SOT/XRT co-alignment of Hinode data is schematically described in Figure 1. Co-aligning the time series of the images from each telescope needs to be performed before co-aligning SOT images with XRT images. The XRT images need to be corrected for both high frequency spacecraft jitter (1–2 arcsec p-p) and orbital distortions associated with the thermal deformations (a few arcsec p-p). We show that the jitter can be removed by applying corrections based on the sun sensor signals with an empirical model for the orbital distortions (section 7). In contrast, the SOT correlation tracker

(Shimizu et al. 2007) removes most of the satellite jitter and orbital variation from the series of SOT images. However, there is a slow drift originating from the gross motion of solar granules seen in the narrow (11×11 arcsec) field of view of the correlation tracker, which can be removed by performing a rigid co-alignment using cross correlation from image to image and then applying the cumulative offsets to the whole time series.

To obtain the best alignment, XRT and SOT need to take regular G-band images. If the images are taken every 10 minutes then co-alignment of less than 1 arcsec can be attained. When sunspots or pores are located in the field of view, they are used as fiducials to co-align the data from the two telescopes with each other. In quiet sun data, there are no clear fiducial marks in 1 arcsec G-band images from XRT, and the calibrated DC pointing offset needs to be used for co-alignment (section 8).

SOT can take images at different wavelengths with its filter imaging capabilities. The Broadband Filter Imager (BFI) produces photometric images with broad spectral resolution in 6 bands at the highest spatial resolution and at rapid cadence. The Narrowband Filter Imager (NFI) provides intensity, Doppler, and full Stokes polarimetric imaging at high spatial resolution. Slight offsets and different magnifications exist between the images at different wavelengths, but they can be co-aligned with calibrated offset and magnification parameters (section 5). SOT has another observing capability, the Spectro-Polarimeter (SP), which obtains line profiles of two magnetically sensitive Fe lines and the nearby continuum while slit scanning a region of interest. The solar features will evolve and move during a fairly long scanning time, but a small portion of the scanning area can be well co-aligned with BFI or NFI images by using the granule patterns and other solar features seen in the continuum.

3. Mercury transit and DC pointing offset

An unique opportunity for obtaining calibration data came about 10 days after opening the protective doors of the telescopes. A transit of Mercury across the solar disk was observed on 8 November 2006. The images acquired in 21:18 - 21:55 UT were used for this calibration. Mercury was seen in 5 successive frames of G-band exposures ($4K \times 2K$ pixels, no pixel summing) by SOT BFI. One of the images taken with SOT is shown in Figure 2 (a). XRT observed the Mercury transit with a lot of X-ray exposures (512×512 pixels, no pixel summing, Al_Poly filter, 16.38 sec exposure duration), four frames of which are shown in Figure 2 (b) to give the movement of Mercury in this period. During this period, only series of X-ray exposures were made, at different focus positions, for evaluating the best focus position using the sharp limb of Mercury.

The position of Mercury can be used to measure the offset between the SOT field of view and the XRT X-ray field of view. Since the size of Mercury is small (10.0 arcsec in diameter), the position of Mercury in each of frames was determined with sub-arcsec accuracy, as shown in Figure 3 (a) and (b). Note that the time stamp in UT was ver-

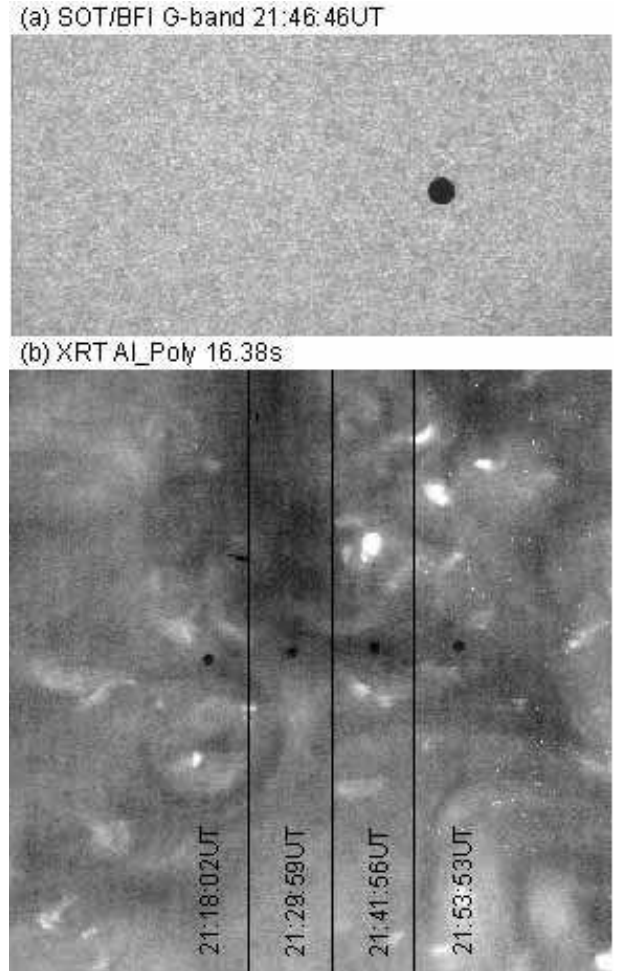


Fig. 2. Mercury transit observed with (a) SOT and (b) XRT on 8 November 2006. The small dark spot in each frame is Mercury.

ified by using the timing of Mercury touching to each of the solar limbs. Satellite jitter as well as orbital variation were removed in XRT data according to the information described in section 7. Active tip-tilt mirror control with correlation tracker (Shimizu et al. 2007) was enabled during the period. At the time between the 3rd and 4th frames, the tip-tilt mirror angle was reset to its home position (note that it is slightly biased due to hysteresis, see Shimizu et al. 2007 for details) because the angle reached the stroke limit, causing a positional jump in the series of SOT images. The magnitude of the positional jump was determined and corrected (4.9 arcsec W, 0.0 arcsec N) by using magnetic patterns that were well observed in Ca II H frames, and that were also acquired in G-band. Figure 4 gives the pointing offset between the XRT X-ray optics and SOT BFI, as determined with the Mercury transit. The center of the XRT X-ray field of view is located 36.6 arcsec east and 23.1 arcsec south of the BFI CCD field of view.

The transit of Mercury also gives the plate scale and orientation of the CCD frames by comparing the measured trajectory on the CCD frames with the predic-

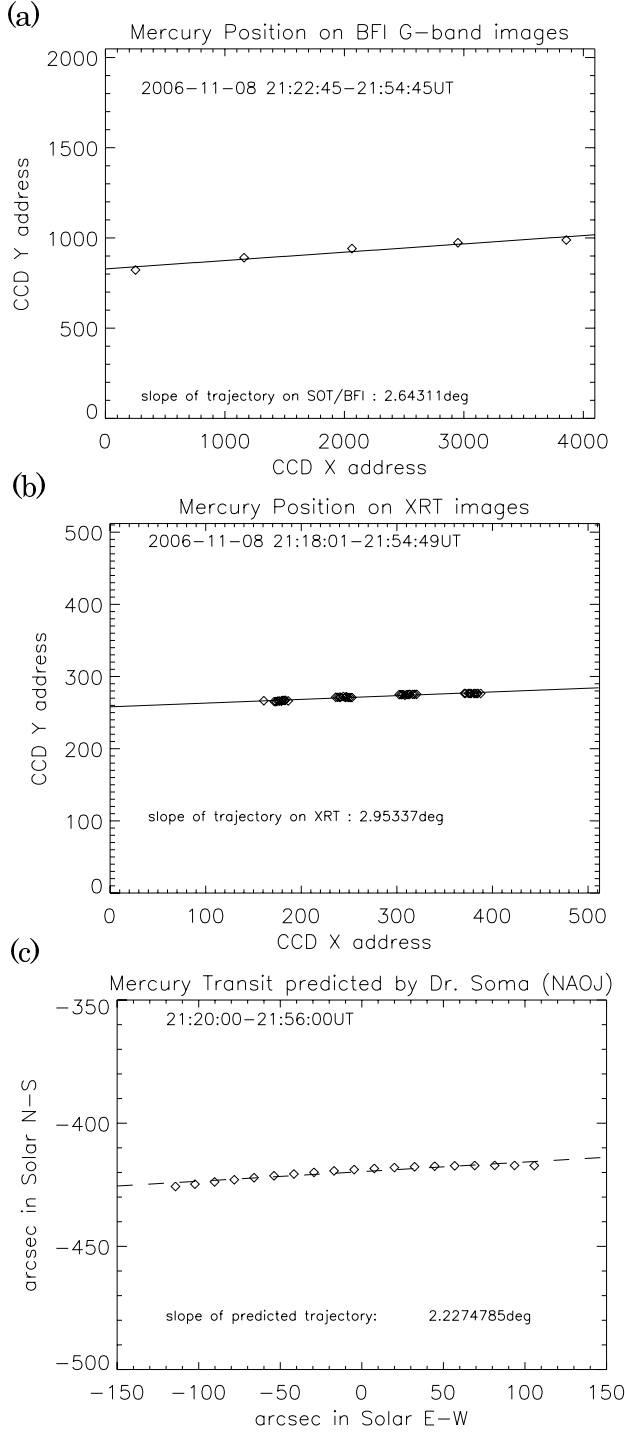


Fig. 3. Trajectory of Mercury on the CCDs: (a) Position of Mercury in SOT BFI G-band $2K \times 4K$ CCD frames. (b) Position of Mercury observed with XRT X-ray Al_KPoly filter 512×512 pixel frames. The CCD positions after performing positional corrections to remove satellite jitter and orbital variation for XRT and tip-tilt mirror angle for SOT. (c) Prediction of Mercury position in the solar heliocentric coordinate seen from the Hinode satellite.

Measured Mercury position
at 2006-11-08 21:46:46.634UT

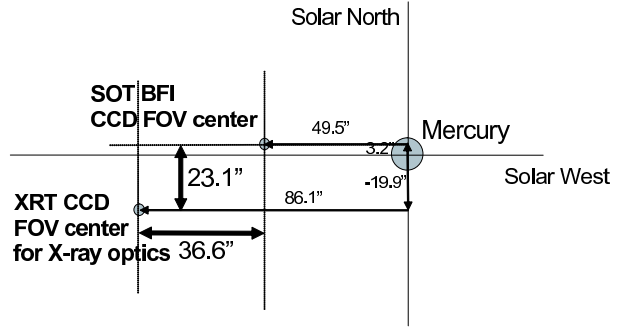


Fig. 4. DC pointing offset between SOT and XRT X-ray images.

tion of the Mercury transit in solar heliocentric coordinate. It is noted that a similar calibration with another Mercury transit was made for the soft X-ray images from the *Yohkoh* satellite (Wülser et al. 1998). Figure 3 (c) is the position of Mercury on the solar disk calculated using orbital elements of the Hinode spacecraft. The plate scale derived from the Mercury transit is as follows:

$$0.0545 \pm 0.0004 \text{ arcsec/pixel for SOT BFI CCD;} \\ 1.031 \pm 0.001 \text{ arcsec/pixel for XRT CCD.}$$

Note that a small uncertainty is included in the measurement for the BFI CCD because of imperfect tip-tilt mirror angle correction. The derived XRT plate scale is in good agreement with the plate scale derived from the fitting to the X-ray limb, which gives $1.031 \pm 0.001 \text{ arcsec pixel}^{-1}$. The data taken on 21 December 2006 at 11:00–14:00 UT gives $951.0 \pm 1.0 \text{ pixel}$ for the radius of the solar dark disk determined by the limb fitting, whereas the radius of the visible-light photospheric sun is 975.45 arcsec at that date. It was also assumed that the radius of the X-ray dark disk is 3500 km larger than that of the visible-light photospheric disk with consideration of the distance from the photosphere to the bottom of the corona. Moreover, another precise comparison can be made to confirm the XRT plate scale (Ishibashi 2007)—the limb position of an XRT X-ray image was co-aligned with the limb of an Fe xv 284\AA image from *SoHO* EIT (Delaboudinière et al. 1996), which plate scale has been well-calibrated. This comparison gives an XRT plate scale statistically consistent with that from the Mercury measurement.

The slope of trajectory observed on each CCD gives the roll angle offset of the frames from the solar north direction. The prediction gives that the slope of the trajectory in the period of 21:20 – 21:55 UT is tilted 2.228 deg from the east-west line. The slope of the Mercury trajectory is tilted 2.643 deg on the BFI CCD frame and is tilted 2.95 deg on the XRT CCD frame. This measurement gives that the BFI CCD frame is offset $0.416 \pm 0.005 \text{ deg}$ clockwise, and the XRT CCD frame is offset $0.73 \pm 0.03 \text{ deg}$ clockwise, both from the solar north direction (Figure 5).

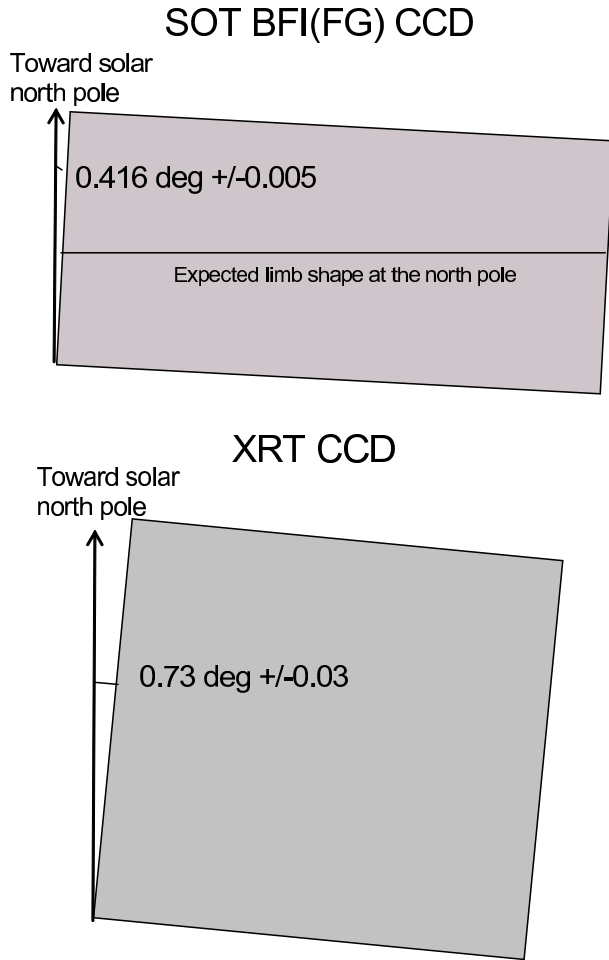


Fig. 5. Roll angle offset of SOT/BFI and XRT CCD frames from the solar north direction.

4. XRT internal offset

The XRT consists of optimized Wolter-I-like grazing incidence soft X-ray optics together with co-focal visible light optics (Golub et al. 2007). Both soft X-ray and visible light images are focused onto a single CCD detector (Kano et al. 2007). G-band images are taken by inserting the glass G-band filter into the focal plane and opening the visible light shutter. This allows light passing through the visible light optic to reach the CCD, and the glass filter is opaque to X-rays. The G-band optical axis has a slight offset from the X-ray optics, although the magnification (plate scale) is same. The offset was measured before launch at the X-Ray Calibration Facility (XRCF) at NASA/MSFC (NASA Marshall Space Flight Center) using an optical light source (Golub et al. 2007). The design of the XRT mirror support plate ensured that the visible light optic and the X-ray mirror remained rigidly fixed through launch.

On orbit we have checked the offset by fitting the solar limb seen in both G-band and X-ray images to determine both the center of the Sun and the radius in CCD pixels. The series of G-band and X-ray images acquired on

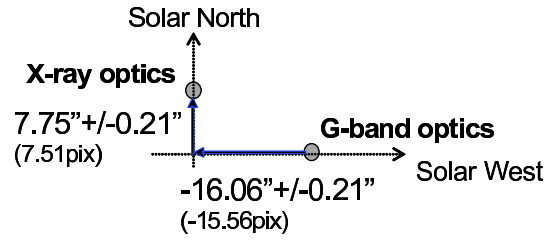


Fig. 6. XRT internal offset of X-ray images from G-band images.

3 March 2007 at 6:05–9:30 UT (22 frames for each) were used. Since it is known that the limb fitting routine used is sensitive to the initial guess, the initial guess was selected to be located roughly at the middle of the travel range due to orbital variation. It was also checked that the initial guess does not change the results even when ± 1 pixel perturbation for (x, y, r) is applied. All the results were matched within < 0.07 pixel. Short-term satellite jitter and orbital drift corrections were applied to the fitting results. The offset of XRT G-band images from X-ray images determined by this study is given in Figure 6. The error of each G-band/X-ray pair is 0.8–0.9 pixel, but 22 pairs of measurements reduce the error to 0.2 arcsec. The alignment between the G-band and X-ray optics is stable; no systematic offset change is associated with orbital phase.

5. SOT internal offset

Slight offset and pixel scale (magnification) differences exist from image to image at different wavelengths. They were evaluated with 6 sets of the images taken at synoptic observations in November 2006 – April 2007, by performing a rigid co-alignment using cross correlation from image to image. Tables 1 and 2 give the derived shift in X (E-W) direction and Y (N-S) direction, and the derived scale deviations, in comparison to BFI G-band images (4305 Å). Table 1 shows that, for example, the field-of-view (FOV) center of Ca II H (3968 Å) full ($4K \times 2K$) frames is located 1.35 pixels east and 5.24 pixels south of the FOV center in G-band full frames, where the pixel unit is the pixel of original Ca II H images before scaling its magnification. Table 2 gives that the FOV center of Fe I line (6302 Å) full frames is 3.4 pixels east and 26.3 pixels north of the FOV center in G-band full frames, where the pixel unit is the pixel of the Fe I images before scaling its magnification. Since NFI has not yet acquired a sufficient number of images at the other wavelengths, the pre-launch evaluation (Okamoto et al. 2007) is given in Table 2. The accuracies of the derived offset and scale differences are estimated to be about 0.2 pixels at the 1σ level and 0.00005, respectively.

The spectro-polarimeter (SP) data needs a careful consideration when it is co-aligned with the BFI and NFI images. Each slit position may contain a small deviation from the ideal scanning step (0.16 arcsec), as shown in Okamoto et al. (2007). Also, the alignment of SP optics

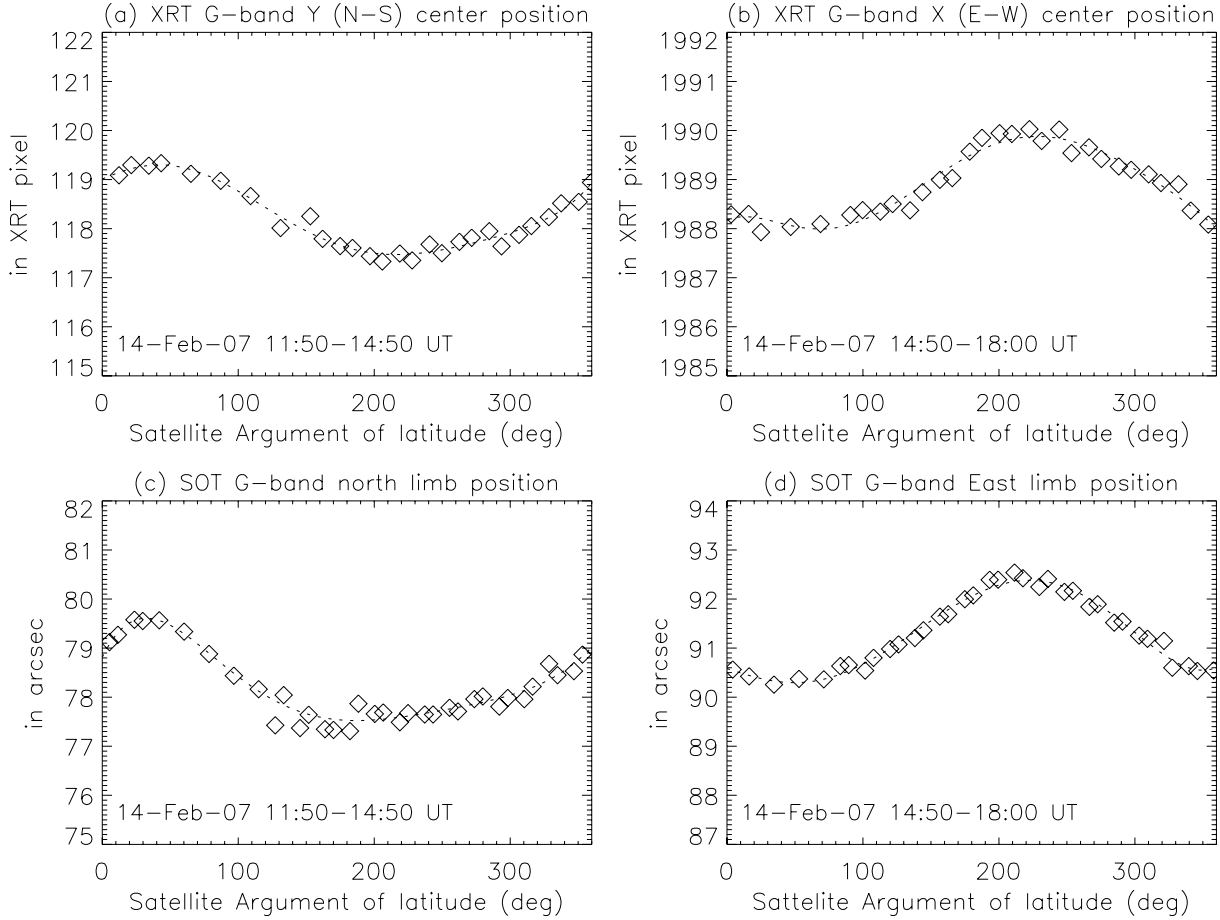


Fig. 7. SOT and XRT pointing direction as a function of orbital phase.

Table 1. BFI Images offset and scale.

wavelength (Å)	xshift ⁽¹⁾ (pix)	yshift ⁽¹⁾ (pix)	xscale ⁽²⁾	yscale ⁽²⁾
3883	0.94	-6.23	1.00041	1.00041
3968	-1.35	-5.24	1.00021	1.00021
4305	0.00	0.00	1.00000	1.00000
4504	1.34	6.49	0.99921	0.99921
5550	-0.36	3.03	0.99497	0.99497
6684	0.60	-1.38	0.99140	0.99140

Note (1): The offset at the center pixel (2047.5, 1023.5) of the full frame (4K×2K) images to the center pixel of G-band (4305) data. The offset is given in the pixel unit of original image at each wavelength before scaling its magnification.

Note (2): Scale deviation from the G-band data. The value larger than 1 means that the pixel scale of original image at each wavelength is larger than that of G-band image.

Table 2. NFI Images offset and scale in reference of G-band (4305) center.

wavelength (Å)	xshift ⁽¹⁾ (pix)	yshift ⁽¹⁾ (pix)	xscale ⁽²⁾	yscale ⁽²⁾
5172*	-6.2	23.9	1.4720	1.4650
5250*	-6.6	23.3	1.4711	1.4642
5576*	-6.2	24.5	1.4699	1.4630
5896*	-8.2	22.1	1.4673	1.4604
6302	-3.4	26.3	1.4660	1.4591
6563*	-2.8	25.9	1.4655	1.4586

Note (1) (2): same as notes in Table 1.

Note *: Not yet evaluated with flight data. Pre-launch data (Okamoto et al. 2007) is shown for reference only.

is significantly sensitive to ambient temperature, and the calibrated level-1 data may still contain positional jitter on the order of about 1 arcsec along the slit, although the calibration performs a correction for the alignment change due to ambient temperature. Moreover, solar features evolve and move during the relatively long period of each map. With these characteristics, accurate co-alignment of SP data with BFI and NFI images would be achieved

only when a rigid co-alignment using cross-correlation is applied to a limited scanning range of the SP data.

6. Pointing drift associated with orbital phase

Each telescope onboard the Hinode spacecraft shows pointing drift on the order of a few arcsec (p-p), which varies as a function of the orbital phase of the satellite. In order to monitor the orbital variation regularly, the team has performed weekly-basis co-alignment measurements since February 2007. These measurements are limb observations to the north and the east, with about 2 hours runtime for each of the limbs. Using the limb seen in the CCD frames from each telescope, we can monitor how the pointing of each telescope behaves with time.

Figure 7 is the orbital drift of XRT and SOT fields of view as a function of satellite latitude, measured on 14 February 2007. Disk center position on the CCD frames is derived from a series of XRT G-band images by limb fitting, whereas the position of the partial portion of the limb seen in each SOT frame is monitored with a series of BFI G-band images. The correlation tracker is disabled, and the tip-tilt mirror is at the home position with accuracy < 0.3 arcsec during the measurements. Pointing jitter induced by the satellite is removed by subtracting sun sensor signal, and therefore the alignment offset of each telescope from one of the sun sensors as the reference is derived. It turned out that the orbital drift of the XRT pointing is quite similar to that of the SOT pointing. The orbital drift is well repeated with the period of the satellite revolution.

7. Satellite jitter and orbital drift correction

Signals from two sun sensors, Ultra Fine Sun Sensors UFSS-A and UFSS-B, can be used to know the jitter induced by the satellite attitude body control. The signals have good accuracy with a random noise level of 0.35 arcsec at the 3σ level. It should be noted that the UFSS sensor signals also contain a gradual orbital drift that depends upon the orbital phase of the satellite. We have established a method (xrt.jitter.pro) to apply a satellite jitter and orbital drift correction to a time series of XRT images by using the sun sensor signals and the information described in section 6. As an example, Figure 8 shows the jitter residual in the time series of XRT G-band images (acquired over about 4 hours) after applying the correction to the image cube. Sunspot position seen in the field of view is given as a function of time. The series of images are stabilized within residual jitter of 1 arcsec (p-p) or better.

8. Long-term evolution of the DC pointing offset

According to the baseline co-alignment method in section 2, the offset between the XRT and SOT data needs to be determined for each dataset. This is because we do not have the information on the tip-tilt mirror angle with sufficient accuracy for subarcsec co-alignment. This

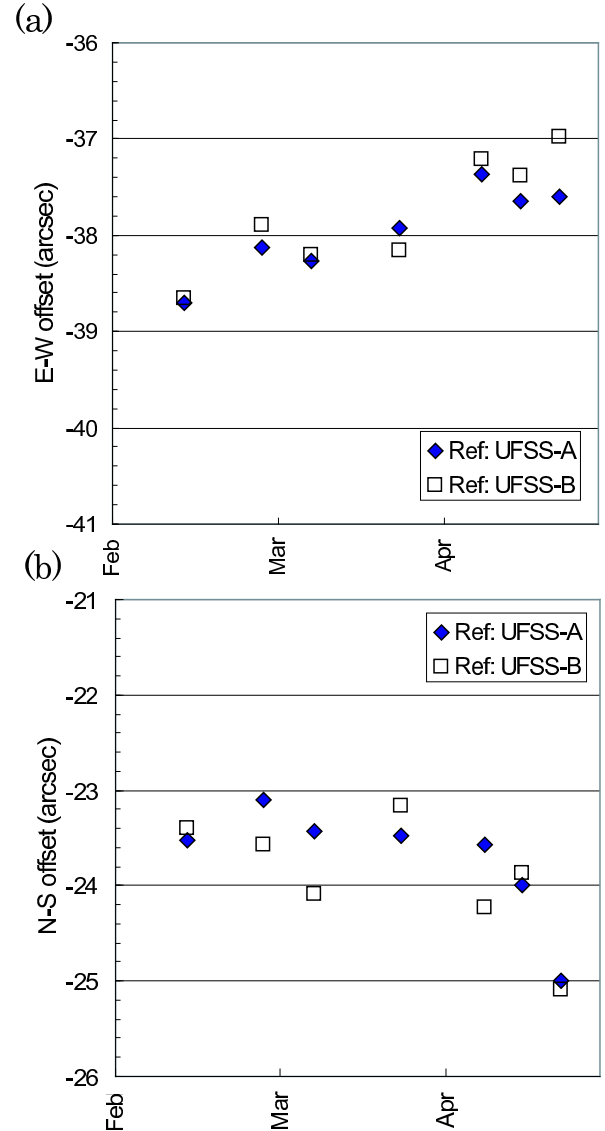


Fig. 9. Long-term change of the pointing offset between SOT and XRT.

method can work very well for active-region observations, in which the position of sunspots in G-band data can be utilized to derive the offset. However, the DC pointing offset value is needed for co-aligning the images of the quiet Sun, which have no fiducial in G-band, although the co-alignment accuracy may be degraded due to uncertainty in the tip-tilt mirror angle. Moreover, XRT did not acquire G-band images regularly during observations at the performance verification phase before early February, so that we need the pointing offset even for some active-region observations.

Since February 2007, co-alignment measurements give how the DC pointing offset changes over long time scales, which is shown in Figure 9. This shows that the offset between XRT and SOT is extremely rigid but that it has slowly drifted about 2 arcsec in both N-S and E-W directions in about 3 months. Note that the absolute values in

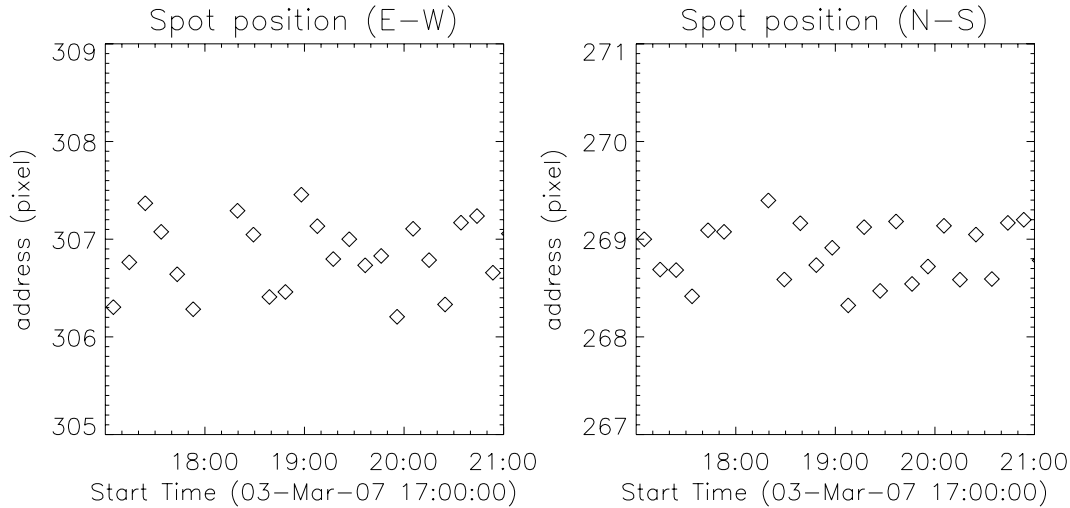


Fig. 8. Sunspot position as a function of time after applying the satellite jitter and orbital drift corrections. The center position of the leading sunspot of NOAA 10944 is derived from the time series of G-band images acquired on 3 March 2007. The pixel unit is 1.031 arcsec.

the figure may contain 1–2 arcsec uncertainty due to systematic error in plate scale, because the center position of the solar disk in the BFI frame coordinate is estimated from the measured position of the partial limb seen in the narrow BFI field of view using the solar radius from the calendar, which is then compared with the center of the solar disk derived from XRT fitted limbs. The comparison of the sunspot position observed both with BFI and XRT G-band data at almost the same time (12 UT on 28 February) gives that the offset in N-S and E-W directions is 24.2 arcsec and 37.9 arcsec, respectively.

After 26 February 2007, a special tip-tilt mirror reset is implemented at the start of correlation tracker operation (CT SERVO ON in observation time line) to minimize the bias caused by hysteresis of the tip-tilt mirror mechanism. This reset ensures that the tip-tilt mirror starts from its home position angle within 0.1 arcsec at the 1σ level.

9. Final remarks

We have evaluated the co-alignment performance of Hinode observational data, especially the co-alignment between SOT and XRT data, and confirmed that co-alignment better than 1 arcsec can be realized between SOT and XRT with our baseline method. The results presented in this paper can be applied to the data acquired before early May 2007, the start of the eclipse season (May – August). The co-alignment performance will be changed significantly during the eclipse season, and the DC pointing offset may be changed before and after the eclipse season. Hinode data users should remember this note.

Hinode is a Japanese mission developed and launched by ISAS/JAXA, with NAOJ as domestic partner and NASA and STFC (UK) as international partners. It is operated by these agencies in co-operation with ESA and

NSC (Norway). The authors would like to express their thanks to all the people who have been involved in design, development, tests, launch operation, and science operations for realizing the Hinode (Solar-B) mission and its new advanced observations presented in this paper. For archiving sub-arcsec co-alignment among the data from the onboard telescopes as one of key technical requirements on the spacecraft design, spacecraft system engineers of Mitsubishi Electric Corp., especially Sadanori Shimada, Toshio Inoue, Norimasa Yoshida, are greatly acknowledged for their efforts on the spacecraft structural and thermal designs.

References

- Culhane, J. L. et al. 2007, *Sol. Phys.*, in press.
- Delaboudinière J.-P. et al. 1996, *Sol. Phys.* 162, 291.
- Golub, L. et al. 2007, *Sol. Phys.*, accepted.
- Ichimoto, K. et al. 2007, *Sol. Phys.*, submitted.
- Ishibashi, K. 2007, private communication.
- Kano, R. et al. 2007, *Sol. Phys.*, submitted.
- Kosugi, T. et al. 2007, *Sol. Phys.*, accepted.
- Okamoto J. et al. 2007, in proceedings of the 6th Solar-B science meeting, K. Shibata, T. Sakurai, S. Nagata, Eds. (Astronomical Society of the Pacific), in press.
- Shimizu, T. et al. 2007, *Sol. Phys.*, submitted.
- Suematsu, Y. et al. 2007, *Sol. Phys.*, submitted.
- Tarbell, T.D. et al. 2007, *Sol. Phys.*, submitted.
- Tsuneta, S. et al. 2007, *Sol. Phys.*, submitted.
- Wülser, J.-P., Hudson, H. S., Nishio, M., Kosugi, T., Masuda, S., and Morrison, M., 1998, *Solar Physics*, 180, 131.